ADVANCED MATERIALS

The current density (J), voltage (V), and luminance (L) characteristics were measured using an HP4145 semiconductor parameter analyzer, with the quantum efficiency obtained by placing and centering the OLEDs onto the surface of a calibrated Si photodiode with a large diameter.

Received: January 19, 2004
Final version: February 19, 2004

[1] J. Kido, K. Nagai Y. Okamoto, *J. Alloys Compd.* **1993**, *192*, 30.
[2] J. Kido, H. Hayase, K. Hongawa, K. Nagai K. Okuyama, *Appl. Phys. Lett.* **1994**, *65*, 2124.
[3] T. Tsutsui, N. Takada, S. Saito E. Ogino, *Appl. Phys. Lett.* **1994**, *64*, 1868.
[4] T. Sano, M. Fujita, T. Fujii, Y. Hamada, K Shibata K. Kuroki, *Jpn. J. Appl. Phys.*, *Part 1* **1995**, *34*, 1883.
[5] R. A. Campos, I. P. Kovalev, Y. Guo, N. Wakili T. Skotheim, *J. Appl. Phys.* **1996**, *80*, 7144.
[6] A. Edwards, C. Claude, I. Sokolik, T. Chu, Y. Okamoto R. Dorsinville, *J. Appl. Phys.* **1997**, *82*, 1841.
[7] L. Liu, W. Li, Z. Hong, J. Peng, X. Liu, C. Liang, Z. Liu, J. Yu, D. Zhao, *Synth. Met.* **1997**, *91*, 267.
[8] X. Zhang, R. Sun, Q. Zheng, T. Kobayashi W. Li, *Appl. Phys. Lett.* **1997**, *71*, 2596.
[9] H. Kanai, S. Ichinosawa, Y. Sato, *Synth. Met.* **1997**, *91*, 195.
[10] Y. Ohomori, H. Ueda, Y. Kurosaka, Y. Hamada K. Yoshino, *Jpn. J. Appl. Phys.*, *Part 2* **1998**, *37*, L798.
[11] M. Uekawa, Y. Miyamoto, H. Ikeda, K. Kaifu T. Nakaya, *Bull. Chem. Soc. Jpn.* **1998**, *71*, 2253.
[12] M. D. McGehee, T. Bergstedt, C. Zhang, A. P. Saab, M. B. O'Regan, G. C. Bazan, V. I. Srdanov A. J. Heeger, *Adv. Mater.* **1999**, *11*, 1349.
[13] C. J. Liang, D. Zhao, C. Liang, X. Liu, J. Peng D. Zhao, *Synth. Met.* **1999**, *104*, 165.
[14] M. A. Baldo, S. R. Forrest, presented at the Material Research Society, Fall Meeting, Boston, MA, December 1999.
[15] C. Adachi, M. A. Baldo S. R. Forrest, *J. Appl. Phys.* **2000**, *87*, 8049.
[16] C. J. Liang, D. Zhao, Z. R. Hong, D. X. Zhao, X. Y. Liu, W. L. Li, J. B. Peng, J. Q. Yu, C. S. Lee S. T. Lee, *Appl. Phys. Lett.* **2000**, *76*, 67.
[17] Y. Kawamura, Y. Wada S. Yanagida, *Jpn. J. Appl. Phys.*, *Part 1* **2001**, *40*, 450.
[18] H. Heil, J. Steiger, R. Schmechel, H. von Seggern, *J. Appl. Phys.* **2001**, *90*, 5357.
[19] Z. R. Hong, C. J. Liang, R. G. Li, W. L. Li, D. Zhao, D. Fan, *Adv. Mater.* **2001**, *13*, 1241.
[20] M. Noto, K. Irie, M. Era, *Chem. Lett.* **2001**, 320.
[21] G. D. Phelan, B. Carlson, X. Jiang, A. K. Y. Jen, L. R. Dalton, *Proc. SPIE-Int. Soc. Opt. Eng.* **2002**, *4809*, 179.
[22] M. A. Díaz-García, S. Fernández De Ávila, M. G. Kuzyk, *Appl. Phys. Lett.* **2002**, *81*, 3924.
[23] C. Y. Yang, V. Srdanov, M. R. Robinson, G. C. Bazan, A. J. Heeger, *Adv. Mater.* **2002**, *14*, 980.
[24] Z. R. Hong, C. S. Lee, S. T. Lee, W. L. Li, S. Y. Liu, *Appl. Phys. Lett.* **2003**, *82*, 2218.
[25] P. P. Sun, J. P. Duan, J. J. Lih, C. H. Cheng, *Adv. Funct. Mater.* **2003**, *13*, 683.
[26] G. D. Phelan, B. Carlson, X. Jiang, A. K. Y. Jen, L. R. Dalton, *Proc. SPIE-Int. Soc. Opt. Eng.* **2003**, *4800*, 683.
[27] F. Liang, Q. Zhou, Y. Cheng, L. Wang, D. Ma, X. Jing, F. Wang, *Chem. Mater.* **2003**, *15*, 1935.
[28] M. R. Robinson, J. C. Ostrowski, G. C. Bazan, M. D. McGehee, *Adv. Mater.* **2003**, *15*, 1547.
[29] Y. Kijima, N. Asai S. Tamura, *Jpn. J. Appl. Phys.*, *Part 1* **1999**, *38*, 5274.
[30] H. Nakada, S. Kawami, K. Nagayama, Y. Yonemoto, R. Murayama, J. Funaki, T. Wakimoto, K. Imai, *Polym. Prepr. Jpn.* **1994**, *34*, 2450.
[31] S. Naka, H. Okada, H. Onnagawa, T. Tsutsui, *Appl. Phys. Lett.* **2000**, *76*, 197.
[32] T. Yasuda, I. Yamaguchi T. Yamamoto, *Adv. Mater.* **2003**, *15*, 293.
[33] M. Latva, H. Takalo, V.-M. Mukkala, C. Matachescu, J. C. Rodrìguez-Ubis, J. Kankare, *J. Lumin.* **1997**, *75*, 149.
[34] S. Sato, M. Wada, *Bull. Chem. Soc. Jpn.* **1970**, *43*, 1955.
[35] M. A. Baldo, C. Adachi, S. R. Forrest, *Phys. Rev. B.* **2000**, *62, 10 967.*
[36] J. Kalinowski, G. Giro, M. Cocchi, V. Fattori, P. D. Marco, *Appl. Phys. Lett.* **2000**, *76*, 2352.

Stamps for Submicrometer Soft Lithography Fabricated by Capillary Force Lithography**

By *Christiaan M. Bruinink*, *Mária Péter*, *Meint de Boer*, *Laurens Kuipers*, *Jurriaan Huskens*,* and *David N. Reinhoudt**

Photolithography has been the main technology for integrated circuit (IC) fabrication during the last few decades,[1] however its extension to the sub-100 nm range requires the development of advanced lithographic techniques, e.g., deep UV and extreme UV photolithography,[2,3] soft X-ray lithography,[4] electron-beam writing,[5] and ion-beam lithography.[6] However, the costs render these techniques less suitable for exploratory research applications, in which requirements such as pattern uniformity, reproducibility, and accurate alignment are not stringent. Complementary non-photolithographic techniques, including soft lithography,[7] nanoimprint lithography (NIL),[8] and capillary force lithography (CFL)[9] have been developed successfully during the last decade in the field of micro- and nanofabrication.

[*] Dr. J. Huskens, Prof. D. N. Reinhoudt, C. M. Bruinink, Dr. M. Péter,
Laboratory of Supramolecular Chemistry and Technology
MESA+ Institute for Nanotechnology
University of Twente
P.O. Box 217, NL-7500 AE Enschede (The Netherlands)
Email: smct@utwente.nl
M. J. de Boer
Transducers Science and Technology group
MESA+ Institute for Nanotechnology
University of Twente
Enschede (The Netherlands)
Prof. L. Kuipers
Strategic Research Orientation 'Advanced Photonic Structures'
MESA+ Institute for Nanotechnology
University of Twente
Enschede ((The Netherlands)
Prof. L. Kuipers
FOM Institute for Atomic and Molecular Physics (AMOLF)
Kruislaan 407, NL-1098 SJ Amsterdam (The Netherlands)

[**] This research was supported by the MESA+ Institute for Nanotechnology and is part of the Strategic Research Orientation 'Advanced Photonic Structures'. Mark A. Smithers of the CMAL/MESA+ is acknowledged for operating the high-resolution SEM.

 © 2004 WILEY-VCH Verlag GmbH & Co. KGaA, Weinheim DOI: 10.1002/adma.200306523

Soft lithography[7] is a versatile and cost-effective patterning technique for the routine fabrication of structures ≥500 nm in size. Soft lithography uses elastomeric poly(dimethylsiloxane) (PDMS) stamps to transfer a relief pattern to the surface of a substrate by conformal contact. High-resolution soft lithography still depends on the availability of advanced lithographic techniques for stamp fabrication.

Several elegant and cost-effective methods for stamp fabrication have been reported by Whitesides and co-workers.[10,11] Their basic strategy is to start from elastomeric PDMS stamps with micrometer-size features and exploit non-photolithographic techniques to fabricate submicrometer-size patterns. Several methods exploit the elastomeric properties of commercial PDMS: microcontact printing (μCP) with stamps under lateral compression,[12] under uniaxial stretching in the plane of the stamp or under vertical pressure normal to the plane of the stamp;[10] or replica molding (REM) against PDMS stamps under lateral compression.[13] These resulted in minimum feature sizes of about 200 nm. Of a greater impact are alternatives like lithographic molding and repetitive REM that combine the facile fabrication of robust high-resolution templates with that of *second-generation* stamps.[14,15]

One technique for fabrication of second-generation masters is capillary force lithography (CFL).[9,16] CFL is an effective patterning technique that employs capillary forces for patterning polymers by combining the essential feature of nanoimprint lithography (NIL)[8]—molding a polymer melt—with the key element of soft lithography[7]—the use of an elastomeric stamp. Of special interest for the fabrication of second-generation masters is CFL of thin (with respect to the intrusion depth of the stamp) polymer layers. The amount of polymer cannot fill the spaces between the stamp and the substrate completely, and this results in the formation of submicrometer-size polymer structures located *at the feature edges* of the original stamp.[9] Recently, Korczagin et al. have shown the CFL of etch resistant polymers (e.g., poly(ferrocenylmethylphenylsilane)) in combination with reactive-ion etching to transfer these edge patterns into silicon.[17] To the best of our knowledge, such polymer or silicon structures have not been exploited as potential masters for high-resolution soft lithography.

Here, we demonstrate a novel soft-lithographic technique by combining CFL and REM for the fabrication of high-resolution, second-generation stamps for soft lithography. It is a two-stage procedure in which CFL is carried out first to fabricate robust high-resolution masters, consisting of submicrometer-size polymer edge structures that are subsequently replicated by REM to generate second-generation PDMS stamps for high-resolution soft lithography. These stamps have been used in different μCP experiments ((+)μCP, (–)μCP and cross-printing) on gold. Subsequent wet chemical etching allowed the fabrication of different patterns in thin layers with a resolution of ~125 nm, without the need for cleanroom facilities.

Figure 1 depicts a schematic representation of our soft-lithographic approach for generating submicrometer-size features in thin gold layers on silicon by μCP. A liquid prepolymer of PDMS (Sylgard 184, Dow Corning Corporation) was cast against a photolithographically patterned master with micrometer-size parallel lines (3 μm width, 5 μm spacing, 1.2 μm depth). The PDMS was cured for 1 h at 60 °C without post-curing in order to obtain stamps of minimal modulus (~0.5 N mm^{-2})[18] suitable for conducting CFL (Fig. 1a). Lee and co-workers[9] have shown that PDMS stamps tend to separate from the substrate during high temperature processing because of differences in thermal expansion coefficients between the stamp and the substrate ($\alpha_{PDMS} \gg \alpha_{Si}$). Therefore, the thickness of the PDMS stamps was kept to only 1 mm in order to ensure sufficient flexibility to prevent separation.

During CFL a meniscus forms at the protruding end of the polymer, which, in the case of polymer insufficiency, results in

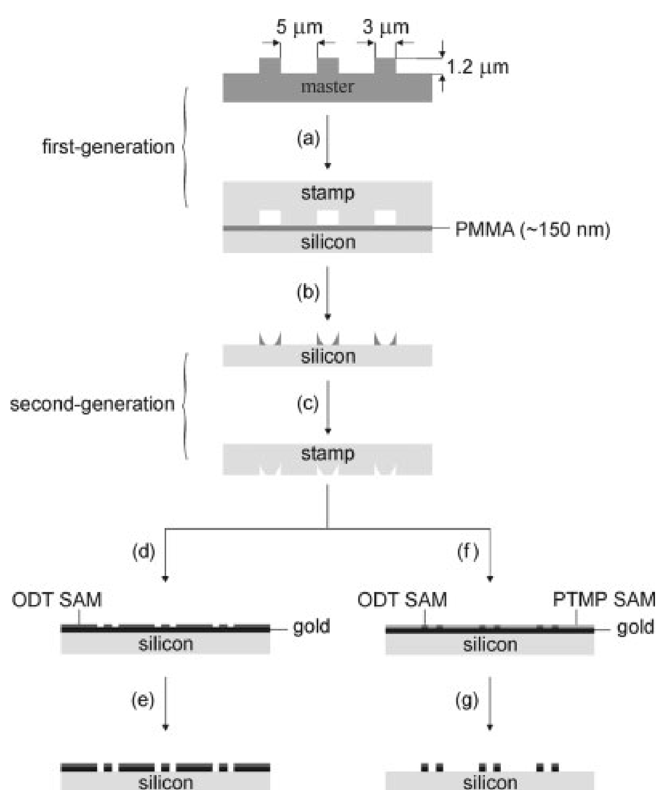

Figure 1. Schematic representation of the fabrication of second-generation PDMS stamps from PMMA templates (i.e., second-generation masters) and the μCP experiments. a) PDMS stamps are fabricated from a master by replica molding (REM) [7]: a prepolymer of PDMS is cast against the master, followed by curing, and release from the master. b) Capillary force lithography (CFL) [9] is carried out on thin PMMA layers. Capillary forces act on the PMMA melt to form patterns specifically along the edges of the original PDMS stamp if the amount of polymer is insufficient to fill the voids between the stamp and the substrate. After cooling to ambient temperature and release of the stamp, the resulting submicrometer-size PMMA edge structures can function, as for example, high-resolution second-generation masters. c) Second-generation PDMS stamps are fabricated from these PMMA masters by REM (as in procedure (a)) and post-cured. d) Microcontact printing with octadecanethiol (ODT). f) Microcontact printing with pentaerythritol-tetrakis(3-mercaptopropionate) (PTMP) and protecting the bare gold by dipping in ODT solution. Selective wet chemical etching of the gold results in trenches in gold ((–)μCP) (e) and gold lines ((+)μCP) (g).

 © 2004 WILEY-VCH Verlag GmbH & Co. KGaA, Weinheim

ADVANCED MATERIALS

submicrometer-size polymer edge structures.[9] Our objective was to exploit these templates as second-generation masters for the fabrication of high-resolution second-generation PDMS stamps. To this purpose, thin poly(methyl methacrylate) (PMMA, $M_w = 38\,000$) layers of ~150 nm were spun onto silicon substrates from a 5 wt.-% solution in toluene. After pre-equilibration of the stamp and the substrate at the annealing temperature, an elastomeric PDMS stamp was brought into conformal contact with the polymer layer.[19] The annealing temperature was set sufficiently above the glass transition temperature T_g (105 °C) in order to ensure polymer mobility for patterning by CFL at 150 °C. Subsequently, the substrate plus the stamp were placed under vacuum at 150 °C for several hours to pattern the polymer layer (Fig. 1b). After cooling to ambient temperature and release of the PDMS stamp, the patterning area and uniformity of the resulting PMMA edge structures were examined by atomic force microscopy (AFM). Cross-section AFM analysis of a representative PMMA master (Fig. 2a) illustrates the excellent uniformity of the master, on which the positions of the ~440 nm high PMMA structures (full width at half maximum (FWHM) is ~680 ± 100 nm) correlate with the periodicity of the PDMS stamp.

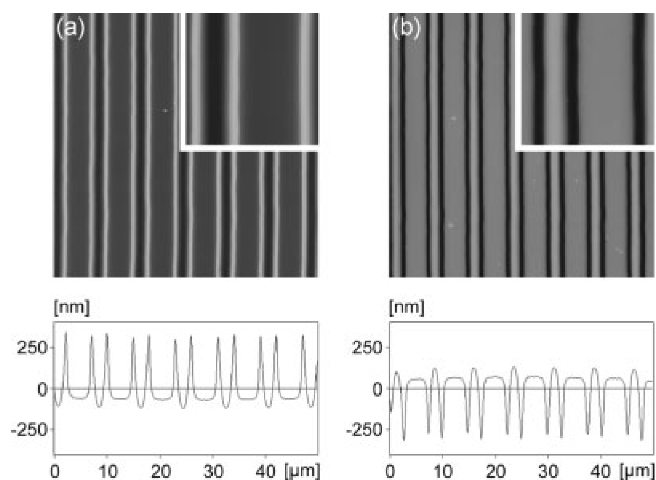

Figure 2. Contact-mode (CM)-AFM height images (z range: 800 nm) of a) the high-resolution second-generation master, and b) the corresponding second-generation PDMS stamp (image size 50 μm × 50 μm), including the corresponding cross-section analysis. The inserts show a close-up detail of the edge structures (image size: 10 μm × 10 μm). The PMMA master was fabricated by CFL with flexible PDMS stamps on a ~150 nm PMMA layer at 150 °C for 6 h in vacuum. Stamp plus substrate were pre-equilibrated at 150 °C for 30 min prior to CFL. Second-generation PDMS stamps were fabricated by casting prepolymer PDMS against the PMMA master and curing for 1 h at 60 °C. Post-curing was done for another 18 h at 60 °C after release of the stamps from the master.

In preliminary CFL experiments, we found that separation is successfully prevented by applying a low pressure (1.6 N cm^{-2}) on regular PDMS stamps or by a gradual increase in temperature to the final annealing temperature in low-modulus and flexible PDMS stamps. However, this resulted in non-symmetric PMMA edge structures. Pre-equilibration of the stamp (with or without post-curing) and the substrate to the annealing temperature before bringing the PDMS stamp in conformal contact with the substrate gave symmetric PMMA edge structures. This procedure is therefore ideal for the fabrication of second-generation masters of PMMA. The remaining irregularities in the width and height of the PMMA edge patterns present in the master most probably originate from dust particles interfering with the alignment of the stamp to the substrate since CFL was carried out outside a cleanroom environment.

The resulting submicrometer-size PMMA masters were replicated in PDMS to generate second-generation stamps (Fig. 1c). Figure 2b shows an AFM image and cross-section AFM analysis of a PDMS stamp, which confirms that REM of our second-generation PMMA masters was achieved with high fidelity, as shown by the ~420 nm deep indentation (FWHM is ~950±100 nm) in the PDMS stamps. The low interfacial free energy, the elasticity of PDMS, and its chemical inertness to PMMA allow for the generation of multiple copies of the PMMA master into second-generation PDMS stamps. No noticeable degradation or damage of the PMMA master was observed after fabrication of more than ten copies.

To illustrate their applicability in soft lithography, the second-generation PDMS stamps were used in μCP (Fig. 1d). μCP of octadecanethiol (ODT) on a 20 nm thick gold layer and subsequent selective wet chemical etching of the gold (Fig. 1e) in an aqueous basic solution containing $K_2S_2O_3$/$K_3Fe(CN)_6$/$K_4Fe(CN)_6$[20] fabricated ~350 nm wide trenches in gold layers (Fig. 3a). Since only the edges of the original (first-generation) master pattern are transferred into the gold layer, our method in combination with μCP and wet chemical etching is an alternative to the general class of edge lithographies.[21–24] The major advantage of our method over existing edge lithographies is that it does not require any cleanroom facilities for the fabrication of the structures.

The discrepancy between the lateral dimensions of the trenches in gold (~350 nm) and the indentations present on the second-generation PDMS stamp (Fig. 2b, cross-section analysis FWHM ~950 nm) suggests that diffusion and deformation of the PDMS stamp during printing contribute to further reducing the feature dimensions.[25,26]

Printing with stamps fabricated from very asymmetric PMMA masters (e.g., by applying pressure on regular PDMS stamps during CFL) and subsequent wet chemical etching resulted in the fabrication of patterns of alternating ~125 nm and ~800 nm wide trenches (Fig. 3b). Although the pattern is not symmetric, it illustrates the potential for printing sub-150 nm features with second-generation stamps consisting of commercial PDMS.

Positive microcontact printing ((+)μCP)[27] with PDMS stamps from the same second-generation master (Figs. 1f,g) gave ~350 nm gold lines (Fig. 3c). (+)μCP was recently developed by IBM to invert the final pattern in gold without the need for new masters.[27] It employs printing with pentaery-

 © 2004 WILEY-VCH Verlag GmbH & Co. KGaA, Weinheim

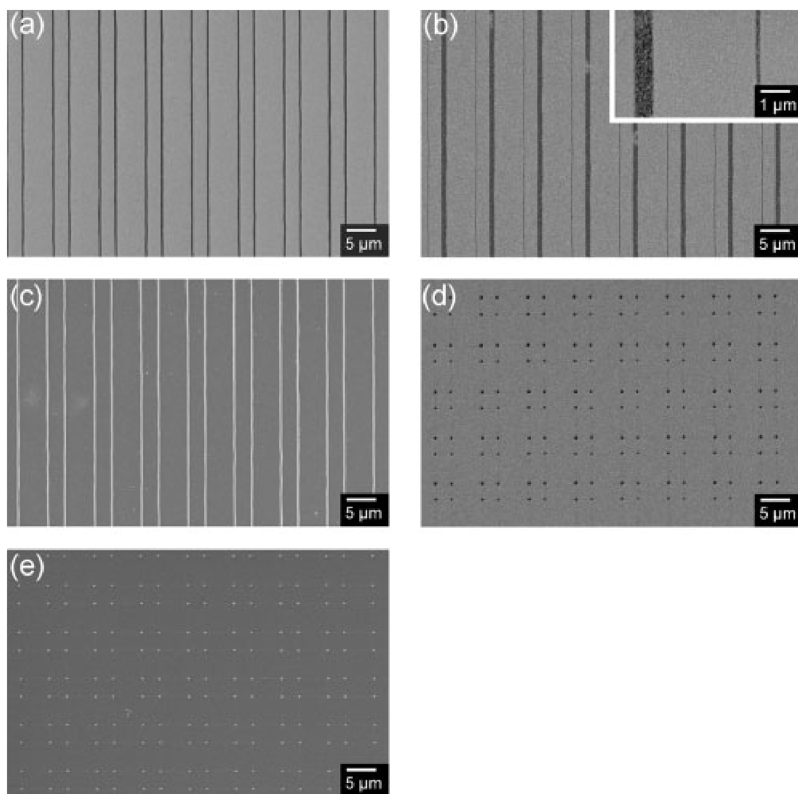

Figure 3. SEM images of different structures generated in a 20 nm gold layer by application of (–)µCP (a,b,d) or (+)µCP (c,e) using second-generation PDMS stamps fabricated from the same PMMA master. Light regions are gold, and dark regions are the underlying Si/SiO_2 substrate. a) Array of ~350 nm wide trenches in gold fabricated by (–)µCP with a stamp inked by 0.3 mM ODT for 60 s, followed by selective wet chemical etching of gold for 7 min. b) Array of ~125 nm wide and ~800 nm wide trenches in gold fabricated by (–)µCP (same conditions) with a PDMS stamp fabricated from an asymmetric PMMA master. c) Array of ~350 nm wide gold lines fabricated by (+)µCP with a stamp inked by 1.8 mM PTMP for 60 s, followed by a 5 s dip in 0.2 mM ODT solution, and selective wet chemical etching of gold for 10 min. d,e) ~350 nm hole/dot grids of gold on silicon fabricated by cross-µCP, i.e., two sequential printing steps on the same substrate with 90° rotation between the prints. The printing time was 30 s for each printing step (1 min in total) and for (+)µCP the stamp was re-inked between the printing steps.

thritol-tetrakis(3-mercaptopropionate) (PTMP), which is compatible with the requirements of µCP, but does not form etch-blocking self-assembled monolayers (SAMs). Adsorption of octadecanethiol (ODT) from solution to the non-contacted areas and subsequent wet chemical etching yields the positive pattern. In our etching experiments we found that PTMP SAMs retard the etching of gold and longer etching was necessary to obtain good-quality patterns.

Cross-printing is a convenient approach to reduce the second lateral feature dimension,[10] and accordingly to increase the inherent low pattern density of our edge lithographic technique. Figures 3d,e illustrate cross-printing with the same stamp and a 90° rotation between the prints.

The 20 nm thick gold patterns are sufficiently robust to serve as secondary etch masks in reactive-ion etching (RIE) of the underlying silicon substrate, resulting in high aspect ratios. Figure 4 shows a cross-sectional scanning electron microscopy (SEM) image of 350 nm wide trenches transferred into silicon using RIE with SF_6/O_2 resulting in 500 nm wide trenches in the silicon. To achieve anisotropic etching of silicon, the black silicon method (BSM)[28] was applied on our etch apparatus prior to etching of the substrates. BSM is an experimental procedure that makes use of the fact that the parameter settings for anisotropic etching are close to the ones for the formation of black silicon.[28] At that point, only minor changes in the parameter settings were done to obtain anisotropic profiles such as the one shown in Figure 4 (anisotropy of ~0.85). Under these RIE conditions, silicon over gold etch selectivity of more than 170 was found.

In summary, we have shown that the combination of capillary force lithography (CFL) and replica molding (REM) is a convenient and inexpensive approach for the fabrication of high-resolution, second-generation PDMS stamps from the corresponding second-generation masters without the need for advanced lithographic techniques. The successful application of these stamps in µCP for the fabrication of ~125 nm features in gold demonstrates its potential to extend the utility of soft lithography in general. The limits of this soft-lithographic method in fabricating symmetric patterns will be explored further. The CFL process has sev-

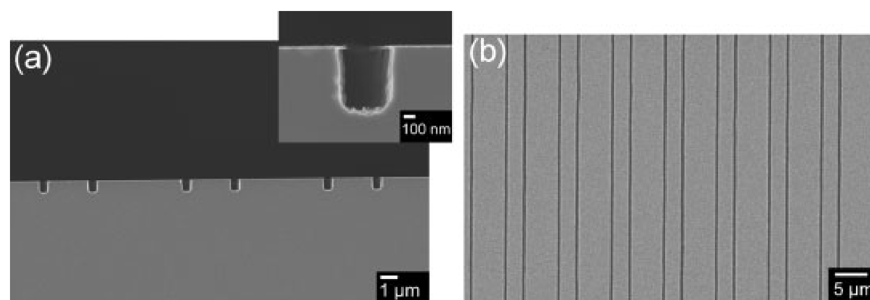

Figure 4. SEM images of linear 500 nm wide trenches transferred 650 nm deep into silicon using SF_6/O_2 RIE (APC open, 50 W radio-frequency (RF) power, 40 sccm SF_6, 20 sccm O_2, and 90 s). Silicon etch rate was about 0.34 $\mu m\,min^{-1}$. a) High-resolution cross-sectional SEM image. The insert shows a clear undercut on the order of 100 nm, resulting in a widening of the silicon trenches with respect to the ones present in the gold mask (350 nm). b) Low-resolution SEM image of the same trenches in top-view.

 © 2004 WILEY-VCH Verlag GmbH & Co. KGaA, Weinheim

eral parameters (e.g., thickness of polymer layer, annealing temperature, stamp fill factor, and annealing time) that can be optimized to reduce the feature dimensions on the master below 100 nm.

Experimental

All experiments were carried out in a regular chemical laboratory. Octadecanethiol (ODT), pentaerythritol-tetrakis(3-mercaptopropionate) (PTMP), EtOH, NaOH, $Na_2S_2O_3$, $K_3Fe(CN)_6$, and $K_4Fe(CN)_6$ were purchased from commercial sources in the highest available purity and used without further purification. A kit of PDMS prepolymer (Sylgard 184 silicone elastomer) and PDMS curing agent (Sylgard silicone elastomer curing agent) was purchased from Dow Corning Corporation. Gold layers (20 nm) on titanium-primed (2–3 nm) silicon wafers were purchased from Ssens BV (Hengelo, The Netherlands).

Stamps were fabricated by casting a 10:1 (v/v) mixture of PDMS and curing agent (Sylgard 184, Dow Corning) against a relief pattern of interest (i.e., silicon master or polymer template), cured for 1 h at 60 °C and released at this curing temperature to avoid build-up of tension due to thermal shrinkage [26b]. PDMS stamps used for μCP were left in the oven at 60 °C for at least 18 h to ensure complete curing.

Silicon substrates of 2 cm × 2 cm were cleaned by ultrasonic treatment in acetone for 15 min, and dried in a continuous stream of nitrogen. PMMA (M_w = 38 000) layers were spun onto the clean silicon substrates at 3000 rpm for 30 s from a 5 wt.-% solution in toluene with minimal delay.

PDMS stamps used for CFL were fabricated by casting against a master with regular lines of 3 μm width, 5 μm spacing, and 1.2 μm depth; and curing for 1 h at 60 °C without additional post-curing in order to obtain very flexible stamps. The thickness of these PDMS stamps was about 1 mm. In order to prevent separation, the PDMS stamps and the polymer layers were equilibrated to the annealing temperature for 30 min prior to bringing the stamp into contact with the polymer layer. The system was left at 150 °C in vacuum for 6 h. After cooling to ambient temperature for 30 min, the PDMS stamps were released from the silicon substrates. The resulting polymer edge structures were used in this case as masters for the fabrication of second-generation PDMS stamps using the common molding and curing procedure.

Gold layers were rinsed with ethanol and dried in a continuous stream of nitrogen. Second-generation PDMS stamps were wet-inked by exposing the stamps to a drop of a solution of ODT or PTMP in ethanol for 1 min. Solvent was removed from the stamps by a continuous stream of nitrogen prior to printing. All printing experiments were carried out by hand, and the print duration was between 30–60 s in all cases. Re-inking of the stamp was done in between printing steps for cross-(+)μCP experiments. (–)μCP: printing with stamps inked with a 0.3 mM solution of ODT. (+)μCP: printing with stamps inked with a 1.8 mM solution of PTMP, followed by a 5 s dip in a 0.2 mM solution of ODT.

After μCP, complete etching of the (bare) gold was achieved by immersing the printed gold substrates in an aqueous solution of 1.0 M NaOH, 0.1 M $Na_2S_2O_3$, 0.01 M $K_3Fe(CN)_6$, and 0.001 M $K_4Fe(CN)_6$ for 7 min at room temperature. [Caution: potassium ferricyanide is light sensitive. Photodecomposition releases products that can contain free cyanide. Potassium ferricyanide is also incompatible with acids and liberates HCN].

Gold patterns were used as secondary etch masks for transferring the pattern into the underlying silicon by reactive ion etching (RIE). RIE experiments were carried out with an Electrotech Plasmafab 310-340 twin deposition/etch system. Anisotropic etching of silicon was achieved using the following conditions: automatic pressure control (APC) open, 50 W, 40 sccm SF_6, and 20 sccm O_2.

PMMA film-thickness determination was carried out with a Plasmos SD 2002 ellipsometer at a wavelength of 632.8 nm. AFM imaging was carried out with a NanoScope III Multimode AFM (Digital Instruments, Santa Barbara, CA, USA) operating in contact mode using Si_3N_4 cantilevers (Nanoprobes, Digital Instruments), with an approximate spring constant of 0.32 N m^{-1}. For height measurements, the scanner was calibrated in the z-direction using a calibration standard with a known step height. Low-resolution SEM imaging was carried out with a JEOL JSM-5610 SEM operating in secondary electron detection mode. High-resolution SEM imaging was carried out with a LEO Gemini 1550 FEG-SEM.

Received: November 25, 2003
Final Version: April 21, 2004

[1] *Handbook of Microlithography, Micromachining and Microfabrication*, *Vol. 1* (Ed: P. Rai-Choudhury), SPIE Optical Engineering Press, Bellingham, WA **1997**.
[2] S. J. Holmes, P. H. Michel, M. C. Hakey, *IBM J. Res. Dev.* **1997**, *41*, 7.
[3] R. H. Stulen, D. W. Sweeney, *IEEE J. Quantum Elect.* **1999**, *35*, 694.
[4] J. P. Silverman, *J. Vac. Sci. Technol. B* **1997**, *15*, 2117.
[5] M. A. McCord, *J. Vac. Sci. Technol. B* **1997**, *15*, 2125.
[6] U. S. Tandon, *Vacuum* **1992**, *43*, 241.
[7] a) Y. Xia, G. M. Whitesides, *Angew. Chem. Int. Ed.* **1998**, *37*, 550. b) Y. Xia, G. M. Whitesides, *Annu. Rev. Mater. Sci.* **1998**, *28*, 153.
[8] S. Y. Chou, P. R. Krauss, P. J. Renstrom, *Science* **1996**, *272*, 85.
[9] K. Y. Suh, Y. S. Kim, H. H. Lee, *Adv. Mater.* **2001**, *13*, 1386.
[10] Y. Xia, G. M. Whitesides, *Langmuir* **1997**, *13*, 2059.
[11] Y. Xia, J. Tien, D. Qin, G. M. Whitesides, *Langmuir* **1996**, *12*, 4033.
[12] Y. Xia, G. M. Whitesides, *Adv. Mater.* **1995**, *7*, 471.
[13] Y. Xia, E. Kim, X.-M. Zhao, J. A. Rogers, M. Prentiss, G. M. Whitesides, *Science* **1996**, *273*, 347.
[14] J. L. Wilbur, E. Kim, Y. Xia, G. M. Whitesides, *Adv. Mater.* **1995**, *7*, 649.
[15] Lithographic molding, for example combines the patterning of gold by microcontact printing (printing and selective wet chemical etching of the bare gold), followed by anisotropic wet etching of silicon in an alcoholic solution of KOH. The resulting V-shaped structures in silicon function as high-resolution masters for stamp fabrication.
[16] K. Y. Suh, H. H. Lee, *Adv. Funct. Mater.* **2002**, *12*, 405.
[17] I. Korczagin, S. Golze, M. A. Hempenius, G. J. Vancso, *Chem. Mater.* **2003**, *15*, 3663.
[18] http://www.zurich.ibm.com/st/microcontact/stamps/material.html
[19] The application of the standard literature CFL procedure (i.e., no pre-equilibration) reported by Lee and co-workers [9] with regular PDMS stamps, (18 h post-curing, > 5 mm thick) resulted in some cases in separation of the stamp from the polymer layer and consequently, in only a small patterning area with symmetric PMMA edge structures.
[20] Y. Xia, X.-M. Zhao, E. Kim, G. M. Whitesides, *Chem. Mater.* **1995**, *7*, 2332.
[21] a) J. A. Rogers, K. E. Paul, R. J. Jackman, G. M. Whitesides, *Appl. Phys. Lett.* **1997**, *70*, 2658. b) T. W. Odom, V. R. Thalladi, J. C. Love, G. M. Whitesides, *J. Am. Chem. Soc.* **2002**, *124*, 12 112.
[22] J. C. Love, K. E. Paul, G. M. Whitesides, *Adv. Mater.* **2001**, *13*, 604.
[23] J. Aizenberg, A. J. Black, G. M. Whitesides, *Nature* **1998**, *394*, 868.
[24] K. E. Paul, T. L. Breen, J. Aizenberg, G. M. Whitesides, *Appl. Phys. Lett.* **1998**, *73*, 2893.
[25] a) E. Delamarche, H. Schmid, A. Bietsch, N. B. Larsen, H. Rothuizen, B. Michel, H. Biebuyck, *J. Phys. Chem. B* **1998**, *102*, 3324. b) L. Libioulle, A. Bietsch, H. Schmid, B. Michel, E. Delamarche, *Langmuir* **1999**, *15*, 300.
[26] a) A. Bietsch, B. Michel, *J. Appl. Phys.* **2000**, *88*, 4310. b) H. Schmid, B. Michel, *Macromolecules* **2000**, *33*, 3042.
[27] E. Delamarche, M. Geissler, H. Wolf, B. Michel, *J. Am. Chem. Soc.* **2002**, *124*, 3834.
[28] H. Jansen, M. J. de Boer, R. J. Legtenberg, M. Elwenspoek, *J. Micromech. Microeng.* **1995**, *5*, 115.

 © 2004 WILEY-VCH Verlag GmbH & Co. KGaA, Weinheim